

**Microphysics of deep tropical convective clouds observed over India, Part 2 :  
simulations with a high resolution spectral bin microphysics model (The HAMP  
contribution)**

**A. P. Khain, D. Rosenfeld, A. Pokrovsky, N. Benmoshe**

The Hebrew University of Jerusalem, Jerusalem, Israel;

**J. R. Kulkarni, and R. S. Maheshkumar**

Indian Institute of Tropical Meteorology, Pune, India

## **1. Introduction**

During summer 2009 a large set of unique in-situ measurements of deep convective clouds over India has been performed within the framework of the CAIPEEX (Cloud Aerosol Interaction and Precipitation Enhancement Experiment) project of the Indian Institute of Tropical Meteorology in Pune, India. The measurements were carried out up to heights of 8 km above the surface. The clouds developed in extremely humid atmosphere. The CCN concentrations were measured as well. In many cases concentration of aerosols was as high as in pyro clouds in the area of biomass burning. In these cases the droplet size distributions were extremely narrow. In spite of extremely high humidity and low cloud base level, high CCN concentrations lead to the fact that first raindrops form at ~ 5.5 km level and the first graupel form at heights of ~ 7 km. In this study the results of simulation of heavily polluted monsoon cloud observed during 24 August 2009 are presented. Calculations were performed using the mixed-phase spectral (bin) microphysics (SBM) Hebrew University Cloud Model (HUCM) with resolution 50 m x 50 m.

## **2. Model description**

The spectral (bin) microphysics Hebrew University Cloud Model (HUCM) described by Khain et al (2008) has been updated in this study to address the issue of turbulent effects on drop collision. The HUCM is a 2-D non-hydrostatic inelastic model in the z-coordinate framework, in which the vorticity and the stream function are used as computational

variables. The model microphysics is based on the solution of the equation system for size distribution functions of cloud hydrometeors of seven types (water drops, plate-, columnar-, and branch-like ice crystals, aggregates, graupel, and hail/frozen drops), as well as the equation system for size distribution function of aerosol particles playing the role of cloud condensational nuclei (CCN). The latter allows simulation of both maritime and continental clouds with different aerosol loadings and distributions. Each size distribution function contains 43 doubling mass bins, the smallest bin corresponding to  $2 \mu m$  radius droplets and the largest bin corresponding to hail-size droplets of  $\sim 6$  cm in diameter. The utilization of such a doubling mass grid provides quite high resolution for description of cloud droplets (drops with radius below  $\sim 22 \mu m$ ), which is the most important feature for our purposes. The model uses precise gravitational collision kernel which increases with height because of the increase in relative particle velocity. To simulate cloud-aerosol interaction, the calculation of the aerosol particles (AP) size distribution function is introduced into the model. The size of dry AP ranges from  $0.005 \mu m$  to  $2 \mu m$ .

The model takes into account the major warm and ice microphysical processes: nucleation of droplets and primary and secondary generation of ice crystals, diffusional growth/evaporation of drops and ice particles, water-water, water ice and ice-ice collisions, freezing/melting, breakup of drops, etc. In order to control the transition of snow (aggregates) to graupel by riming, the snow bulk density was calculated for each mass bin. If the bulk density exceeded  $0.2 gcm^{-3}$ , i.e. became close to that of graupel, the snow from this bin was converted into a graupel belonging to the graupel bin of the same mass. To determine the snow bulk density in each mass bin, the rimed fraction of snow in each bin was calculated. Accordingly, an additional size distribution describing the rimed mass within each snow bin was introduced. The mass fraction of frozen water within each snow bin was recalculated in the course of water-snow, snow-snow and snow-crystal collisions.

To calculate the parameters adequately characterizing turbulent cloud structure, the following model improvements were made. First, *the model resolution was increased*, so the resolution of 50 m in both the horizontal and the vertical direction was used instead of the standard model resolution of 250 m x 125m. One can expect that the grid increment of 50 m falls within the inertial turbulence sub-range. Thus the scales irresolvable by the model grid are turbulent scales, which is in contrast to the case of a cruder resolution when subgrid scales include both turbulent scales and a certain range of convective scales. This resolution makes the HUCM close to LES models. Second, *the calculation of turbulent parameters is included at each time step in each grid point*.

Several parameters characterizing cloud turbulence were calculated: the turbulence kinetic energy  $E$ , the turbulent viscosity coefficient  $k$ , dissipation rate  $\varepsilon$  and the Taylor microscale Reynolds number  $Re_\lambda$ . The values of  $\varepsilon$  and  $Re_\lambda$  were used for determination of turbulent induced collision enhancement factor using lookup tables presented by Pinsky et al (2008). As a result the changes of size distributions due to collisions were calculated by solving the stochastic collision equation with turbulent collision kernel which is equal to the gravitational kernel multiplied by the collision enhancement factor depending of space and time. The procedure of calculation of the turbulent collision kernel is described in Khain et al (2010) in more detail.

### 3. **Experimental design**

Deep convective cloud measured in situ on 24 August 2009 near the Arabian Sea coast was chosen for simulation. Sounding showed a very high humidity, so cloud base was located at ~800m. Concentration of APs playing the role of cloud condensational nuclei (CCN) was extremely high:  $10600 \text{ cm}^{-3}$  at 1% of supersaturation.

The dependence of CCN concentration on supersaturation is shown in Figure 1.

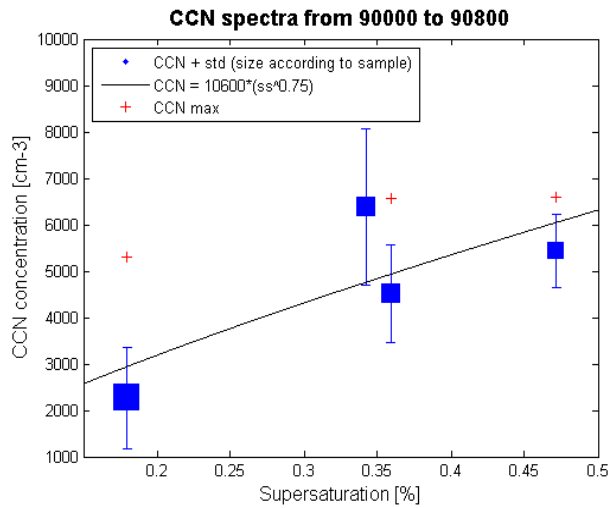


Figure 1. Dependence of CCN concentration on supersaturation as measured below cloud base at 24 August 2009.

Accordingly, the initial size distribution of CCN was calculated using the observed dependence:

$$N_{ccn} = 10600 \cdot S^{0.75} \quad (1)$$

This calculation was performed using the approach described by Khain et al (2000).

Mass distributions measured at different heights in this cloud are shown in Figure 2.

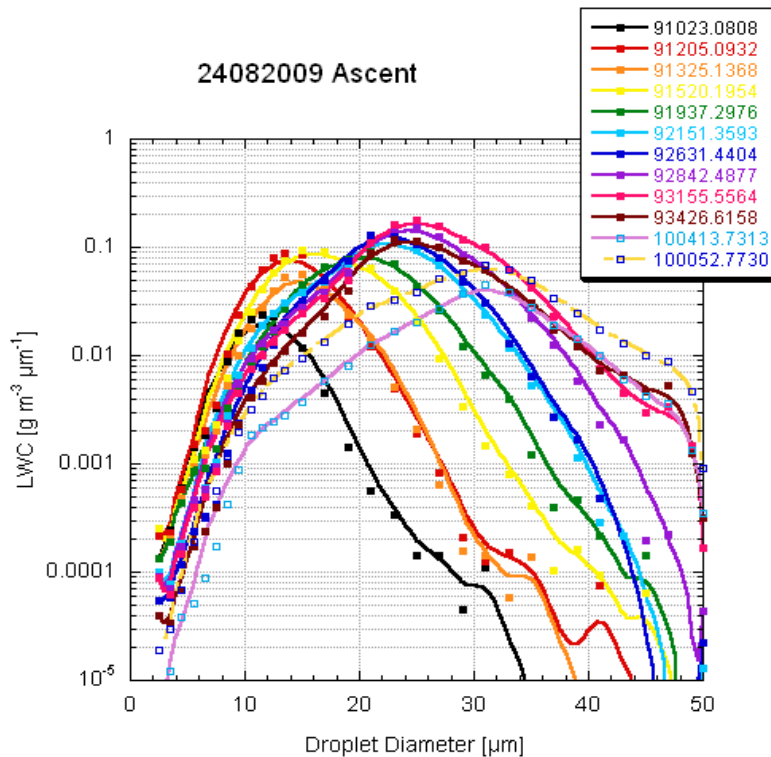


Figure 2. Mass distributions measured in situ in developing cloud observed on 24 Aug. 2009.

One can see that up to height  $\sim 4.7$  km the mass distributions do not contain droplets exceeding  $25 \mu\text{m}$  in radius. The formation of first raindrops can be seen only at height of 5.5 km.

Two simulations were performed 1) with gravitational collision kernel; and b) with turbulent collision kernel, when effects of turbulence of droplet collisions were taken into account.

The cloud was triggered by a weak temperature heating near the surface within the area of 3 km depth.

#### 4. Results of simulations

**Figure 3** shows mass distribution functions calculated using gravitational (left) and turbulent (right) collision kernels.

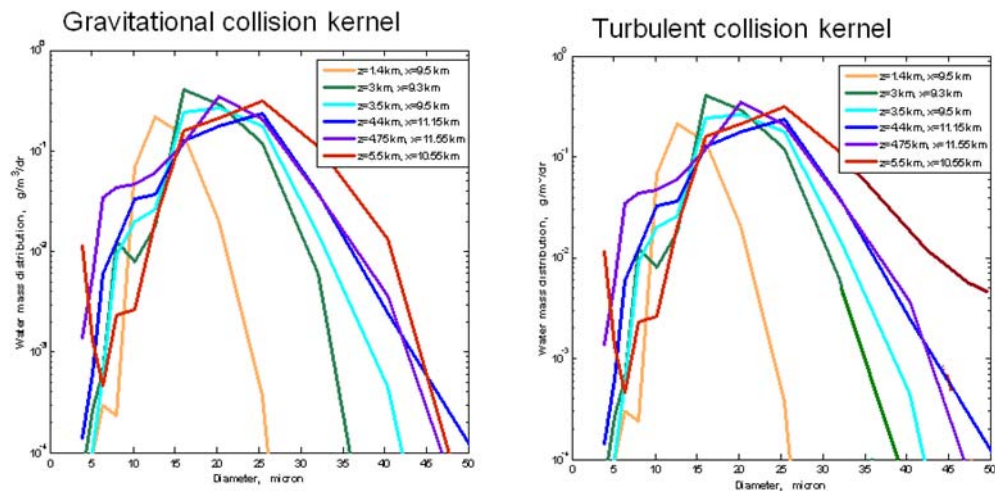


*Figure 3 shows mass distribution functions calculated using gravitational (left) and turbulent (right) collision kernels.*

Comparison with Fig. 2 shows that the model reproduces well the observed size distributions and their evolution with height. At the same time, in the simulations with gravity collision kernel large drop did not form at 5.5 km, while the utilization of the turbulent collision kernel makes the spectrum of droplets wider at heights above  $\sim 4.75$  km. Formation of first raindrops is clearly seen in the right panel by a rapid increase in the concentration of large cloud droplets at  $z=5.5$  km.

Several next figures illustrate cloud microphysical fields at different stages of cloud evolution as simulated by the model. **Figure 4** shows fields of vertical velocity, Cloud water content (CWC), rain water content (RWC) and total ice content (TIC) at  $t=2220$  s

corresponding the beginning of formation of first raindrops. One can see that first raindrops form at  $z=5-5.5$  km and first ice forms at  $z\sim 7$  km in agreement with in-situ measurements. Note a very high maximum values of CWC  $\sim 6-7 \text{ gm}^{-3}$ . Thus, high concentration of AP leads to delay in formation of warm rain and to very high values of CWC.

**Figure 5** shows the same fields by the mature and decaying stage of cloud evolution. One can see that CWC reaches the levels of 9 km. In these cloud bubbles droplets arise due to in-cloud nucleation of CCN. Cloud ice reaches 10 km. Rain is partially due to warm process and partially due to melting of cloud ice.

**Figure 6** shows microphysical fields characterizing ice microphysics: *graupel*, *snow*, *hail* and *ice crystal mass contents* at the mature stage of cloud evolution.

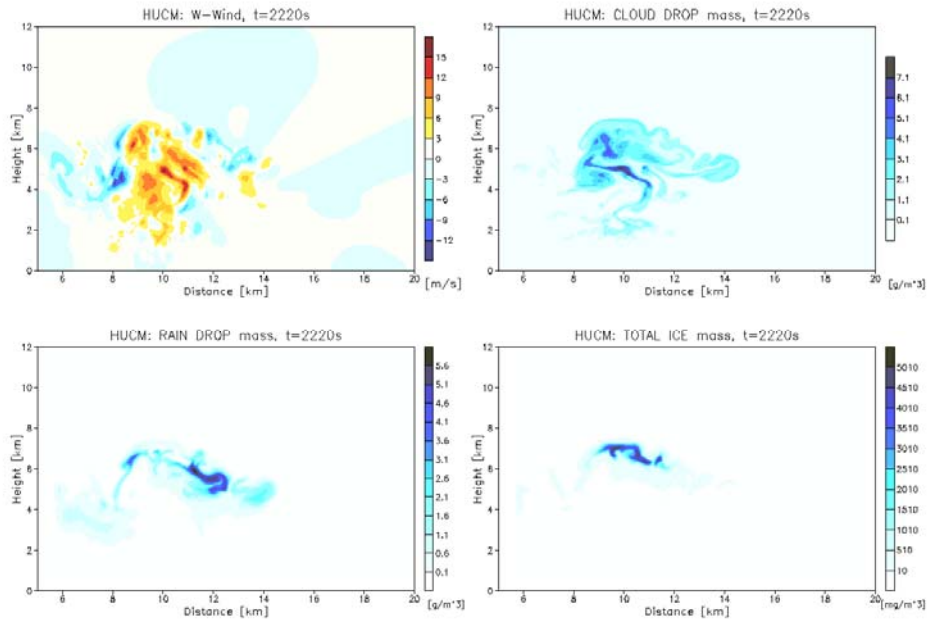


**Figure 4** Fields of vertical velocity, Cloud water content (CWC), rain water content (RWC) and total ice content (TIC) at  $t=2220$  s corresponding the beginning of formation of first raindrops. One can see that first raindrops form at  $z=5-5.5$  km and first ice forms at  $z\sim 7$  km in agreement with in-situ measurements.

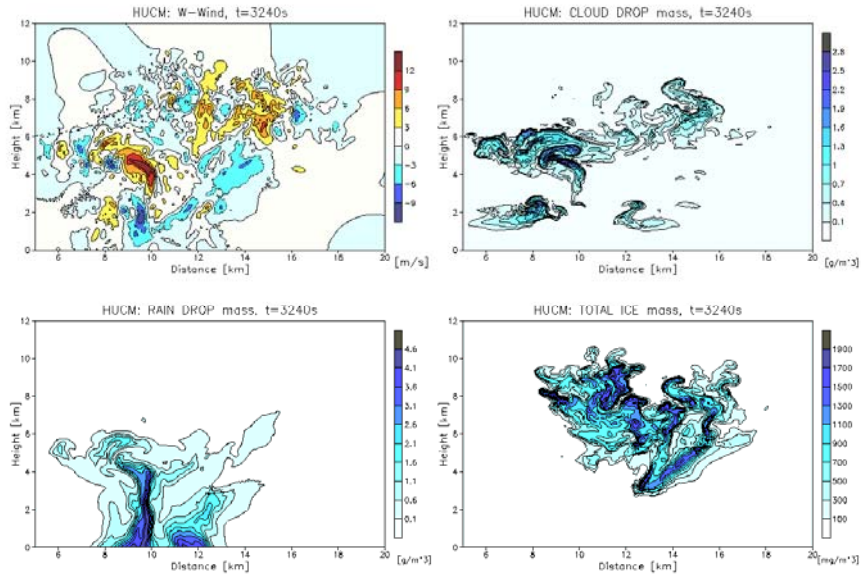


**Figure 5.** The same as in Figure 3, but at the mature and decaying stage of cloud evolution. One can see that CWC reaches the levels of 9 km. In these cloud bubbles droplets arise due to in-cloud nucleation of CCN. Cloud ice reaches 10 km. Rain is partially due to warm process and partially due to melting of cloud ice.

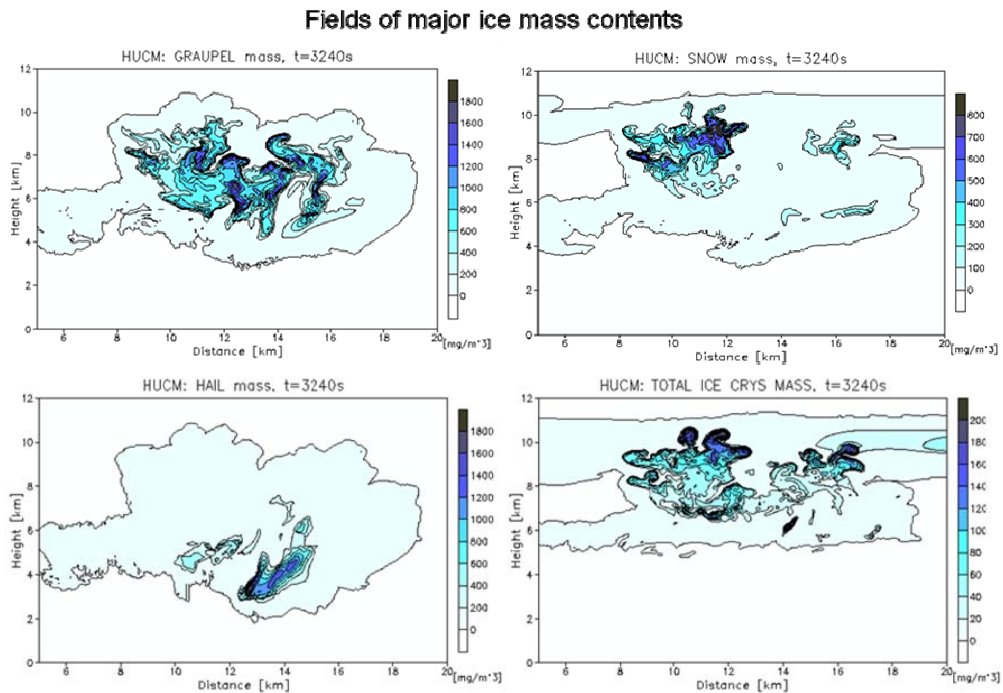


**Figure 6.** Fields of graupel, snow, hail and ice crystal mass contents at the mature stage of cloud evolution.

One can see that the simulated clouds contain comparatively low amounts of ice hydrometeors. Hail forms only as a result of transformation of graupel to hail. We suppose

that this effect is related largely to comparatively low vertical velocities on the simulated cloud.

At last **Figure 7** shows the fields of radar reflectivity and differential radar reflectivity (as could be measured by polarimetric radar). One can see that maximum radar reflectivity does not exceed 55 dBZ, indicating comparatively small sizes of raindrops and lack of large hail. Following rain form a Zdr column. Continuous increase in Zdr downward at x=12-14 km reflects the process of ice melting and formation of raindrops forming large Zdr signal (because of asymmetry of raindrops).

Radar reflectivity and differential radar reflectivity calculated for a deep convective cloud observed 24 Aug. 2009

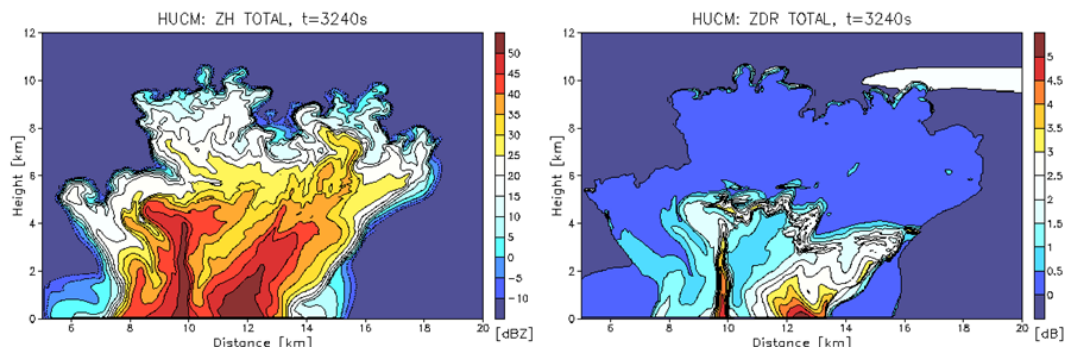


*Figure 7 shows the fields of radar reflectivity and differential radar reflectivity (as could be measured by polarimetric radar).*

## 5. Conclusions

It is shown that the SBM model with resolution of 50x 50 m reproduces size distribution functions measured in situ in extremely polluted clouds with high accuracy. It is also shown the only accounting for turbulent effects on droplet collisions allows one to explain formation of the first raindrops at 5.5 km. In the case when gravitational kernel was used, the raindrops in simulations formed higher that it was observed. The level of ice formation is also well reproduced in the model.

Thus, the model was able to simulate a unique cloud developing in extremely wet atmosphere, but with a dramatic delay in the formation raindrops because of extremely high CCN concentration.

Simulations show that the simulated clouds contain relatively low amount of ice, especially graupel and hail. Supposedly this is the reason of very weak lightning activity in monsoon clouds.

We plan to simulate also pre-monsoon clouds in which vertical velocities are higher and lightning is more intense.

The numerical simulations presented indicate that the model with spectral bin microphysics is able to reproduce these unique in-situ measurements, so that the TC model



based on this microphysics can serve as a benchmark one for investigation of aerosol effects on TC structure and intensity as well as for calibration of different bulk-parameterization schemes.

#### *Acknowledgements*

The study was performed under support of the HAMP program and CAIPEEX.

#### References

- Khain, A. P., M. Ovtchinnikov, M. Pinsky, A. Pokrovsky, and H. Krugliak, 2000: Notes on the state-of-the-art numerical modeling of cloud microphysics. *Atmos. Res.* 55, 159-224.
- Khain A., N. Cohen, B. Lynn and A. Pokrovsky, 2008: Possible aerosol effects on lightning activity and structure of hurricanes. *J. Atmos. Sci.* 65, 3652-3667.
- Khain A., M. Pinsky, N. Benmoshe, and A. Pokrovsky. Turbulent effects on cloud microstructure and precipitation of deep convective clouds as seen from simulations with a 2-D spectral microphysics cloud model, *J. Atmos. Sci.* (in press)
- Pinsky M., A. Khain and H. Krugliak, 2008: Collisions of cloud droplets in a turbulent flow. Part 5: Application of detailed tables of turbulent collision rate enhancement to simulation of droplet spectra evolution. *J. Atmos. Sci.* , 63, 357-374